

Open Source Antibiotics - Simple Diarylimidazoles are Potent Against Methicillin Resistant Staphylococcus Aureus.

Dana M. Klug¹, Edwin G. Tse¹, Daniel G Silva^{1,2}, Yafeng Cao³, Susan A. Charman⁴, Jyoti Chauhan⁵, E. Crighton⁴, Maria Dichiaro⁵, Chris Drake⁶, David Drewry^{7,8}, Flavio da Silva Emery², Lori Ferrins⁵, Lee Graves⁹, Emily Hopkins⁶, Thomas A. C. Kresina⁵, Álvaro Lorente-Macías^{9,10,11}, Benjamin Perry¹², Richard Phipps⁶, Bruno Quiroga⁵, Antonio Quotadamo^{5,13}, Giada N. Sabatino¹, Anthony Sama¹⁴, Andreas Schätzlein¹, Quillon J. Simpson⁵, Jonathan Steele⁶, Julia Shanu-Wilson⁶, Peter Sjö¹², Paul Stapleton¹, Chris Swain¹⁵, Alexandra Vaideanu¹, Huanxu Xie³, William Zuercher⁷, Matthew H. Todd^{1,16*}

¹ School of Pharmacy, University College London, 29-39 Brunswick Square, London WC1N 1AX, United Kingdom.

² School of Pharmaceutical Sciences of Ribeirão Preto, University of São Paulo, Ribeirão Preto, São Paulo, 14040-903 Brazil.

³ WuXi AppTec Company Ltd., 666 Gaoxin Road, East Lake High-Tech Development Zone, Wuhan 430075, People's Republic of China.

⁴ Centre for Drug Candidate Optimisation, Monash Institute of Pharmaceutical Sciences, Monash University, Parkville, VIC 3052, Australia.

⁵ Department of Chemistry and Chemical Biology, Northeastern University, Boston, Massachusetts 02115, United States of America.

⁶ Hypha Discovery, 154b Brook Dr, Milton, Abingdon OX14 4SD, United Kingdom.

⁷ UNC Lineberger Comprehensive Cancer Center, School of Medicine, University of North Carolina at Chapel Hill, Chapel Hill, NC, 27599, USA

⁸ Structural Genomics Consortium, UNC Eshelman School of Pharmacy, University of North Carolina at Chapel Hill, Chapel Hill, NC, 27599, USA

⁹ Department of Pharmacology, University of North Carolina at Chapel Hill, Chapel Hill, NC 27599, USA

¹⁰ Department of Medicinal & Organic Chemistry and Excellence Research Unit of "Chemistry Applied to Biomedicine and the Environment", Faculty of Pharmacy, University of Granada, Campus de Cartuja s/n, 18071 Granada, Spain

¹¹ A. L-M. Present address: Cancer Research UK Edinburgh Centre, Institute of Genetics & Cancer, University of Edinburgh, Edinburgh EH4 2XR, United Kingdom

¹² Drugs for Neglected Diseases *initiative* (DNDi), 15 Chemin Camille-Vidart, 1202 Geneva, Switzerland

¹³ *Clinical and Experimental Medicine PhD Program, University of Modena and Reggio Emilia, 41121 Modena, Italy*

¹⁴ Citizen scientist.

¹⁵ Cambridge MedChem Consulting, 8 Mangers Lane, Duxford, Cambridge CB22 4RN, United Kingdom

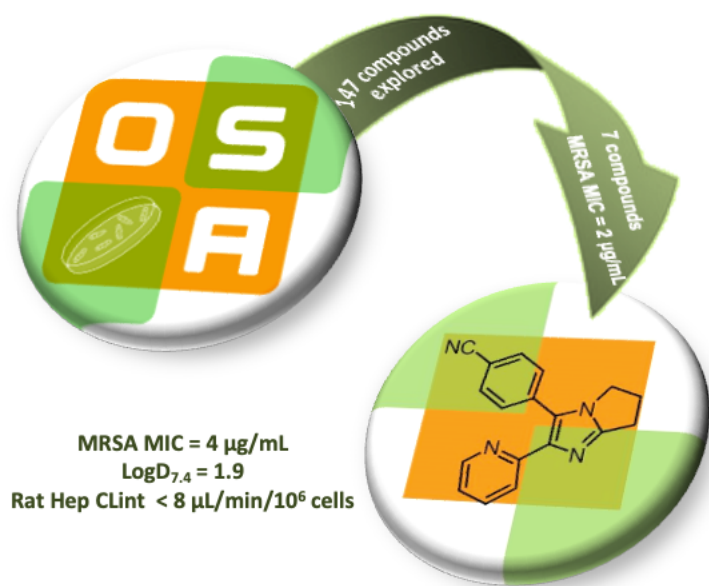
¹⁶ Structural Genomics Consortium, University College London, 29-39 Brunswick Square, London WC1N 1AX, United Kingdom

*Corresponding author: matthew.todd@ucl.ac.uk

Abstract

Antimicrobial resistance (AMR) is widely acknowledged as one of the most serious public health threats facing the world, yet the private sector finds it challenging to generate much-needed medicines. As an alternative discovery approach, a small array of diarylimidazoles was screened against the ESKAPE pathogens (<https://en.wikipedia.org/wiki/ESKAPE>) and the results made publicly available through the Open Source Antibiotics (OSA) consortium (<https://github.com/opensourceantibiotics>). Of the 18 compounds tested (at 32 µg/mL), 15 showed >90% growth inhibition activity against MRSA alone. In the subsequent hit-to-lead optimization of this chemotype, 147 new heterocyclic compounds containing the diarylimidazole and other core motifs were synthesized, tested against MRSA and structure-activity relationships identified. While potent, these compounds have moderate to high intrinsic clearance and some associated toxicity. The best overall balance of parameters was found with OSA_975, a compound with good potency, solubility and reduced intrinsic clearance in rat hepatocytes. We have progressed towards the knowledge of the molecular target of these phenotypically active compounds, with proteomic techniques suggesting TGFRB1 is potentially involved in the mechanism of action. Further development of these compounds towards antimicrobial medicines is available to anyone under the licensing terms of the project.

Graphical Abstract



Introduction

Antimicrobial resistance (AMR) is widely acknowledged as one of the most serious public health threats facing the world.¹ The problem may have been worsened by the overuse of antibiotics to treat COVID-19 patients during the pandemic.² Unfortunately, those antibiotics rendered ineffective by resistance are not being replaced at the rate that society needs. Of the 43 antibiotics in clinical development as of December 2020, only six have the requisite activity against World Health Organization (WHO) critical or Centers for Disease Control and Prevention (CDC) urgent pathogens, and only ten represent a novel class or target.³ This shortfall is primarily due to the high cost of antibiotic development and the challenges of creating a market structure in which novel antibiotics are both stewarded responsibly and made profitable.⁴

In this environment, an open source model for drug discovery can offer several advantages.⁵ A project adopting this approach lacks secrecy: it takes place publicly in real time, with all communication in the public domain, and is not based on a patent model.⁶ Such an approach allows for the recruitment of diverse scientific expertise (freedom to operate is clearly delineated through the use of a Creative Commons licence), reduces or eliminates unproductive duplication of effort and enables a competitive yet collaborative assessment of strategies to solve a problem. While such a model has been previously applied to other discovery projects towards, for example, antimalarials⁷ (<https://github.com/OpenSourceMalaria>) and antifungals,⁸ (<https://github.com/OpenSourceMycetoma>) the project described herein is an example of an open source drug discovery framework applied to the challenge of novel antibiotic discovery.

In an effort to discover new leads against high-priority pathogens, a small array of diarylimidazoles was screened using the Community for Open Antimicrobial Drug Discovery (CO-ADD) platform,⁹ which profiled the compounds against the ESKAPE pathogens *Escherichia coli*, *Klebsiella pneumoniae*, *Acinetobacter baumannii*, *Pseudomonas aeruginosa*, methicillin-resistant *Staphylococcus aureus* (MRSA) and the fungi *Candida neoformans* and *C. albicans*. Of the 18 compounds tested (at 32 µg/mL), 15 showed >90% growth inhibition activity against MRSA but not the other pathogens (Figures S1 and S2, Supplementary Information - Biology). MRSA is a gram-positive pathogenic bacterium that was designated a high-priority pathogen by the WHO.^{1d} AMR was one of the greatest public health concerns prior to the COVID-19 pandemic; only MRSA infections increased by 13% from 2019 to 2020.¹⁰ Given the potential public health benefits (particularly of narrow-spectrum antibiotics on host health,¹¹ we decided to pursue hit-to-lead optimization of this series, which is exemplified by **OSA_822**ⁱ (MRSA active) and **OSA_812** (MRSA inactive) shown in **Figure 1**.

ⁱ In this paper, the numbering of the compounds retains the numbering used in the online Open Source Antibiotics project, maintaining the connection between data in this paper and the live research. Molecules in Open Source Antibiotics are numbered according to a convention described online (https://github.com/opensourceantibiotics/OSA_Tech_Ops/wiki/Molecule-Numbering-Convention) and in the Supplementary Information. In the rest of this paper, the prefix “OSA_” is omitted.

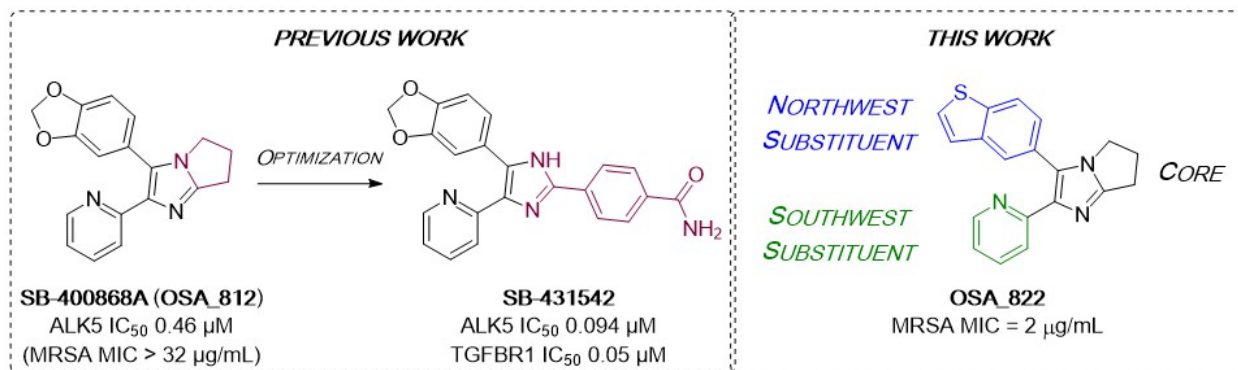


Figure 1. Literature optimization of diarylimidazole SB-400868A to generate ALK5 inhibitors and structure of a representative compound investigated in this work (**OSA_822**) towards compounds potent vs. MRSA.

The chemotype was of previous interest because of a screen of a GlaxoSmithKline internal library collection for inhibitors of the transforming growth factor β 1 (TGF- β 1) type I receptor (ALK5), where compound **812** displayed an IC₅₀ of 0.46 μM against ALK5 and no inhibition of p38 kinase. Optimization led to the selective inhibitor SB-431542 (IC₅₀ 94 nM against ALK5 and still no inhibition of p38 kinase, CC₅₀ > 30 μM), which inhibits TGF- β 1-induced fibronectin mRNA formation (IC₅₀ 0.05 μM) while displaying no measurable cytotoxicity in a 48 hour XTT assay (CC₅₀ > 30 μM).¹²

The promising activity against MRSA, and the low cytotoxicity observed in the ALK5 research, stimulated us to pursue a new hit-to-lead campaign. Three regions of the main scaffold were modified: the bicyclic imidazole core (black), the “northwest” aryl substituent (blue), and the “southwest” aryl substituent (green). Diversification of these motifs, as well as their linkages, formed the basis of our synthetic studies of this chemotype. The aim was to generate potent compounds with promising physicochemical properties and improved metabolic stability while maintaining an acceptable toxicity vs. mammalian cells.

Results and Discussion

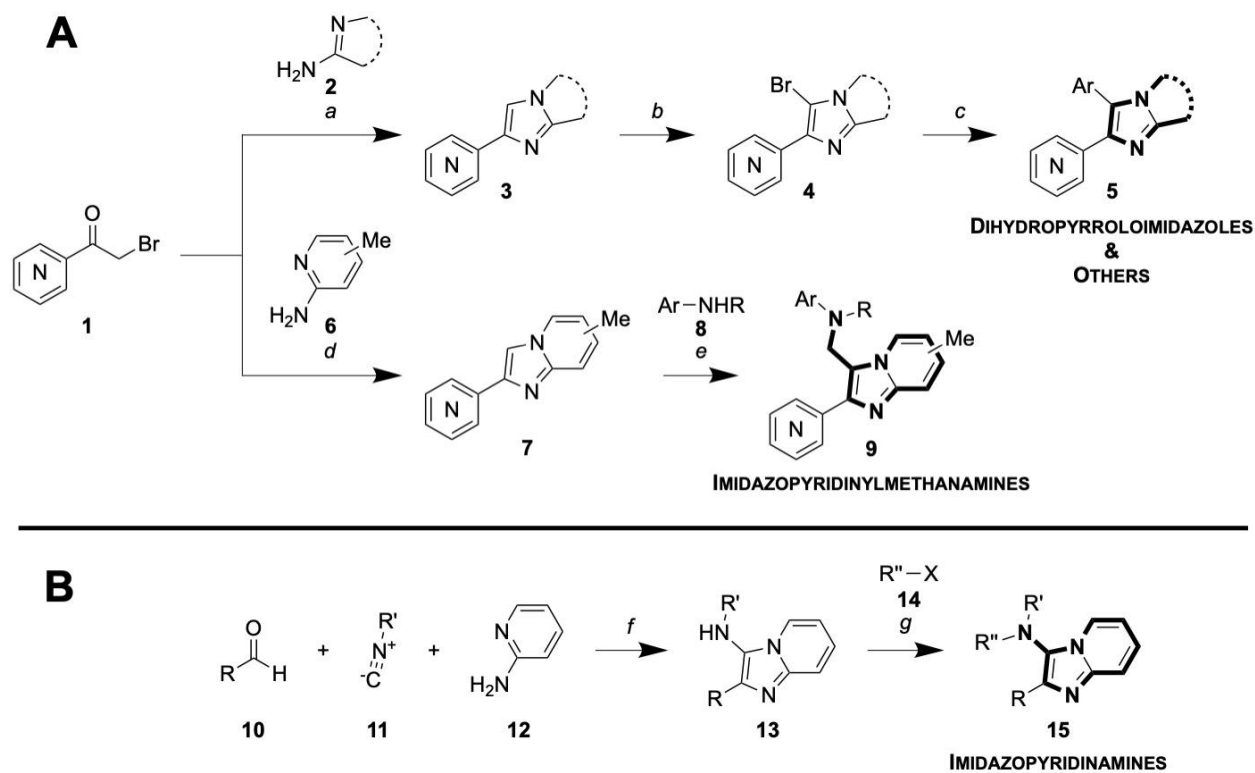
Synthesis

Most compounds synthesized for this campaign followed a general three-step route (**Scheme 1, A**); all chemical experiments are available in full in the relevant “live” online electronic laboratory notebooks as well as in snapshot copies archived in an electronic university repository.¹³ The starting α -bromoketones **1** were cyclized with the desired 2-amino heterocycles **2** to afford fused bicycles **3** that were brominated at the 5-position of the imidazole ring to give **4**. Final compounds **5** were synthesized using standard Suzuki coupling conditions under either conventional or microwave heating.

Several analogues were made with a methylene linker between the core and the aryl amine substituent (**9**). These were prepared *via* an analogous method, starting with a condensation-cyclization of the appropriate α -bromoketone **1** and aminopyridine **6** to give the imidazopyridine core **7**. A Mannich reaction allowed the aminoalkylations necessary for the imidazopyridine

derivatives **9**;¹⁴ some anilines that were used in this reaction (**8**) were alkylated prior to the Mannich step (see Supplementary Information – Chemistry).

Nitrogen-linked analogues were accessed *via* a one-pot Yb(OTf)₃ catalyzed Groebke-Blackburn-Bienaymé reaction with aldehyde **10**, isonitrile **11** and aminopyridine **12** to afford compounds **13**.¹⁵ This was followed, if desired, by nucleophilic substitution with an alkyl halide **14** using Cs₂CO₃ to yield *N*-alkylated compounds **15** (**B**, Scheme 1).



Scheme 1. A) Synthetic route to general (aryl-aryl linkage) analogues. a) **2**, DMF, 100 °C, 18 h; b) NBS, DCM, rt, 1 h; c) ArB(OH)₂ or ArB(pin), Na₂CO₃, Pd(PPh₃)₄ or PdCl₂(dppf)CH₂Cl₂, 3:1 PhMe:EtOH, 120 °C, 18 h (conventional heating) or 30 mins (μW reactor); d) **6**, NaHCO₃, MeOH, reflux, 12 h; e) **8**, formalin (37% aq.), acetic acid, DCM, 18 h. B) Synthetic route to *N*-linked analogues. f) Yb(OTf)₃, 120 °C, 30 mins (μW reactor); g) **14**, Cs₂CO₃, DMF, rt, 18 h. A phenyl ring containing a central “N” denotes a general (aza)aromatic. Yields are described in Supplementary Information – Chemistry.

Structure-activity relationships

In total 147 compounds have been evaluated in this study. The most significant molecules – those that contribute most to an understanding of the SAR – are reported below, but all molecules are described in the Supplementary Information and may additionally be found in the online project infrastructure (<https://github.com/opensourceantibiotics/Series-2-Diarylimidazoles>). Twenty-four compounds were donated by the Drugs for Neglected Diseases *initiative* (DNDi) for which the experimental data have been published.¹⁶ An additional 36 compounds were contributed from Northeastern University, the experimental details for which may be found in a separate publication

that has been recently accepted;¹⁷ the compound identities are delineated in the Supplementary Information – Biology, Tables S1 and S2.

We began our SAR investigations by preparing a wide variety of analogues with variation in the northwest aryl substituent; the aim was to capitalize on the potency of the benzothiophene of **822** while reducing the potential metabolic liabilities of that motif.¹⁸ As shown in **Figure 1**, several fused bicycles were tolerated; of note is the “reverse” (6-substituted) thiophene **830** that was found to be almost equipotent to the original compound **822** (unlike the less potent 3-substituted analogue **832**) and the benzofuran pair **821** and **829** that were similarly potent. Compounds with bicyclic motifs containing unsaturated rings were found to be ineffective (e.g., **827/828**), as were aromatic nitrogen-containing fused bicycles (e.g., benzothiazoles **835** and **836**, quinoline **833**).

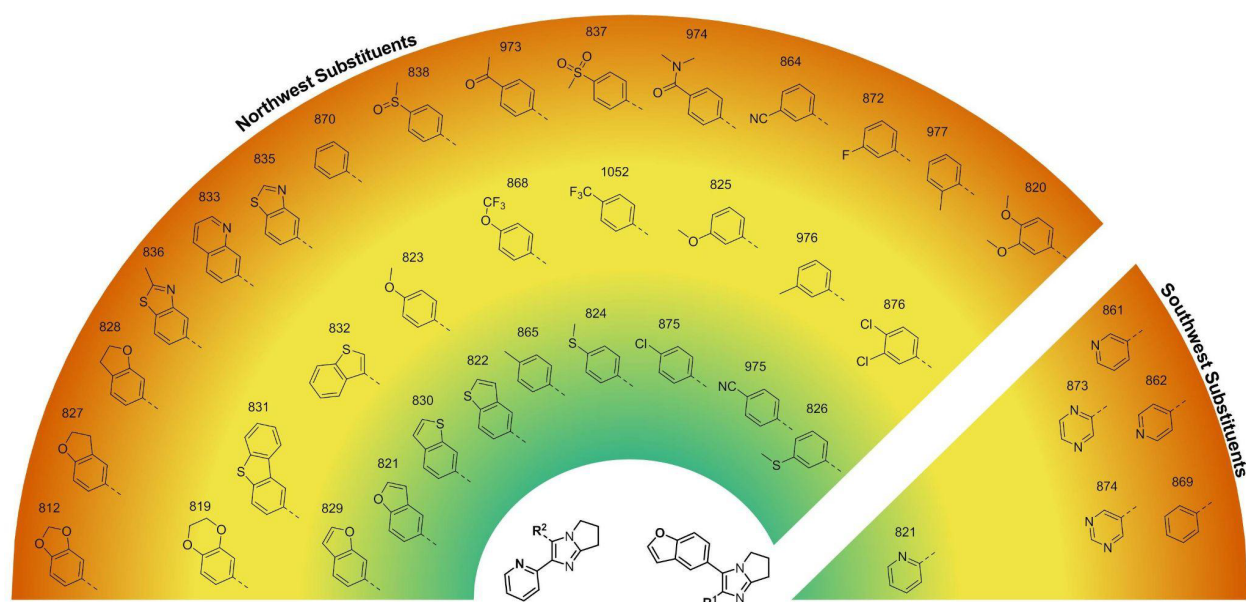


Figure 1. Heat map of *in vitro* potency against MRSA of analogues with variations in the northwest and southwest substituents. Color gradient: green < 4 µg/mL; yellow < 16 µg/mL; red = 32 µg/mL.

We additionally explored a variety of simpler, substituted phenyl rings at the northwest position. Replacement of the benzofuran moiety in **821** with *para*-tolyl (**865**, green region) maintained potency; other *para*-substituted phenyl rings (e.g., in **824**, **875**, and **975**) resulted in significantly improved activity against MRSA when compared to the analogue with an unsubstituted phenyl ring (**870**). Small alterations to the *para*-substituent significantly influenced potency (e.g., **824** vs. **838**), though a group in this position generally performed better than the same group in the *meta* position (e.g., **865** vs. **976**, **975** vs. **864**). A focused library based on the promising compound **975** was synthesized and evaluated (Table S2, Supplementary Information – Biology) but none of the compounds retained the potency of the parent. More oxidized substituents, such as acyl (**973**), methyl sulfone (**837**), or dimethylamide (**974**), were not tolerated (**Figure 1**, red region).

We rapidly established the essentiality of the southwest 2-pyridyl substituent: unlike compound **821**, pyridine isomers **861** and **862** were inactive, as were the unsubstituted phenyl compound (**869**) and the pyrazines **874** and **873**.

Our SAR investigations then focused on evaluation of fused aromatic cores (**Figure 2**). Compounds **859** and **986**, containing a benzo-fused core and a northwest aromatic moiety, were inactive, but the potency could be mitigated by fine-tuning of the substituents (e.g., *p*-Me (**1018**) or *p*-(NEt₂) (**1011**)) and, interestingly, the introduction of a nitrogen atom spacer in compound **987** that was seen as promising because of the introduction of a sp³ nitrogen providing an additional point of diversity and potentially better solubility. This compound was explored through variation of other coordinating rings in the southwest (**1022**, **847**, **1008** and **1009**) with no improvement in potency.

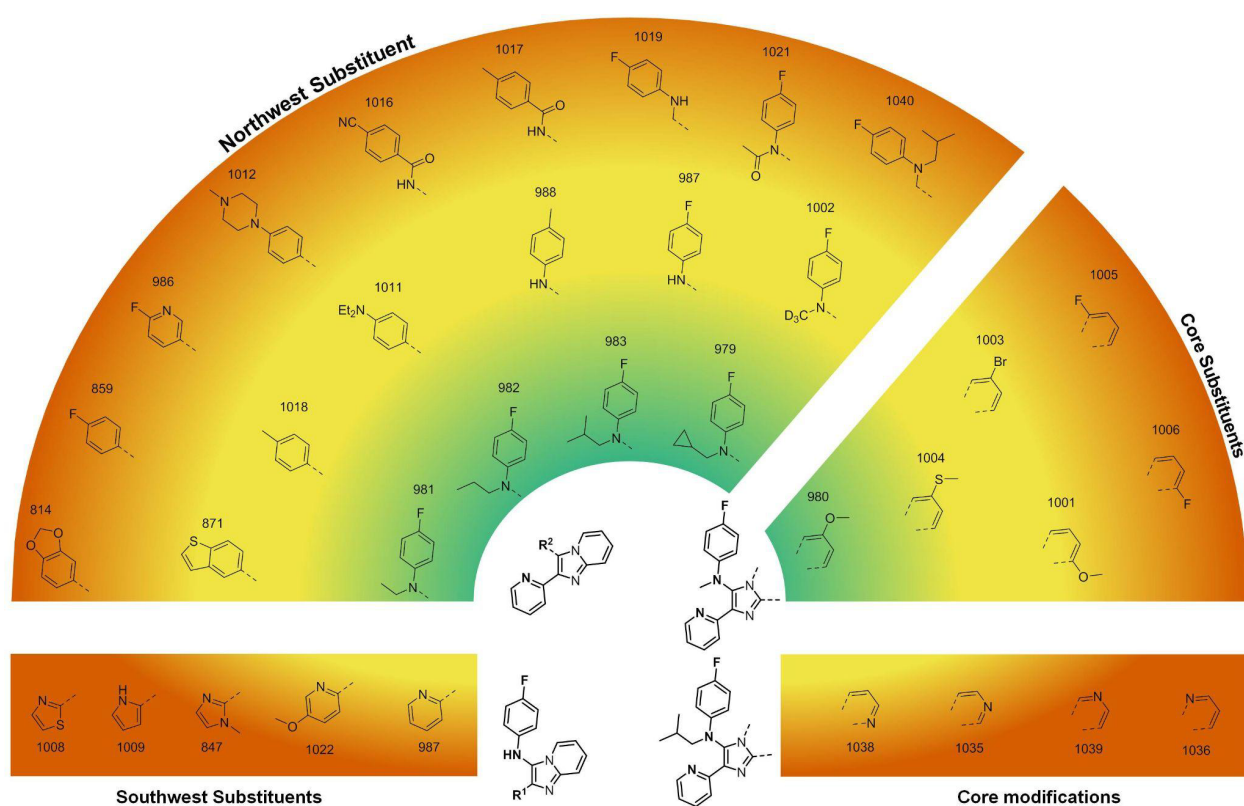


Figure 2. Heat map of *in vitro* potency against MRSA of analogues containing fused bicyclic cores. Color gradient: green < 4 µg/mL; yellow < 16 µg/mL; red = 32 µg/mL.

Acylation (**1021**) or homologation (**1019**) of the amine provided no benefit, but a significant improvement in potency was seen with alkylation of the nitrogen atom (**979**, **981–983**). While maintaining this motif, it was found that some substitutions were acceptable on the fused aromatic core (e.g., 6-methoxy in **980**) though with a high degree of sensitivity to such substitutions (e.g., lower potencies seen with structurally close isomers (**1001**) or analogues with other minor changes (**1003–1006**)). While it was hoped the use of an aza-aromatic ring in the fused core might

help with solubility, a nitrogen atom in any of the four available positions on that ring (*i.e.*, **1035**, **1036**, **1038**, **1039**) was deleterious to potency. An obvious final structure to explore, 1,2-disubstituted benzimidazole, was briefly explored but provided only inactive compounds (Table S2, Supplementary Information – Biology).

Due to the lack of antibiotics for the treatment of multidrug-resistant enterococcal infections, we also tested selected compounds against vancomycin-resistant enterococcus (VRE; Tables S1 and S2). Of these, **979** and **982** showed potent MICs (MIC = 4 µg/mL) against VRE.

From the above campaign that aimed to optimize potency of this series against MRSA, 147 heterocyclic compounds were synthesized and tested, of which 88 were inactive (MIC > 32 µg/mL), 11 were moderately active (MIC = 16 µg/mL) and 43 displayed promising potency (MIC ≤ 8 µg/mL).

ADME and Pharmacokinetics

To guide our initial SAR exploration work, we obtained liver microsomal intrinsic clearance data for five of the initial 18 compounds assayed by CO-ADD (Supplementary Information – CDCO Report and Supplementary Information – Biology). We then acquired intrinsic clearance, plasma protein binding, and solubility data on further compounds throughout the SAR campaign (Tables S3 and S4, Supplementary Information – Biology). Our target was to identify compounds with promising characteristics for lead development: MIC < 4 µg/mL, aqueous solubility ≥ 10 µM, Chrom Log $D_{7.4}$ values below 2, mouse liver CL_{int} < 9.0 µL/min/mg protein, rat hepatocyte CL_{int} < 5 µL/min/10⁶ cells and human plasma protein binding (PPB) ≤ 95%. The data for selected compounds (full data are available in the Supplementary Information) show that these compounds have moderate to high intrinsic clearance (**Figure 3**). The more polar compounds (lower LogD) had reduced PPB and were more metabolically stable. In general, potency was negatively correlated with polarity and solubility, in that the most potent compounds were poorly soluble.

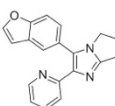
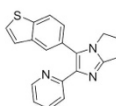
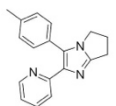
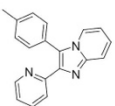
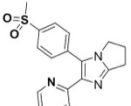
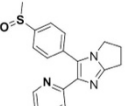
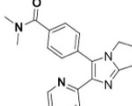
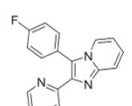
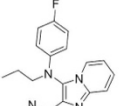
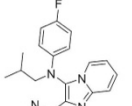
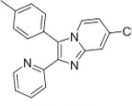
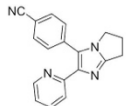
 <p>OSA_821</p> <p>MRSA MIC = 4 µg/mL Aq. Sol. = 117 µM LogD_{7.4} = 2.7 PPB = 97.2%</p> <p>HLM CLint = 63.5 µL/min/mg protein Rat Hep CLint = 13.6 µL/min/10⁶ cells</p>	 <p>OSA_822</p> <p>MRSA MIC = 2 µg/mL Aq. Sol. = 3 µM LogD_{7.4} = 2.9 PPB = 97.7%</p> <p>HLM CLint = 61.5 µL/min/mg protein Rat Hep CLint > 300 µL/min/10⁶ cells MRC5 TC₅₀ = 0.5 µg/mL PMM TC₅₀ = 0.6 µg/mL SI MRC5 < 0 SI PMM < 0</p>	 <p>OSA_865</p> <p>MRSA MIC = 4 µg/mL Aq. Sol. = 32 µM LogD_{7.4} = 2.7 PPB = 92%</p> <p>HLM CLint = 82.0 µL/min/mg protein Rat Hep CLint = 49.2 µL/min/10⁶ cells MRC5 TC₅₀ = 0.4 µg/mL PMM TC₅₀ = 0.6 µg/mL SI MRC5 < 0 SI PMM < 0</p>	 <p>OSA_1018</p> <p>MRSA MIC = 4 µg/mL Aq. Sol. = 43 µM LogD_{7.4} = 3.3 PPB = 99%</p> <p>HLM CLint = 122 µL/min/mg protein Rat Hep CLint = 57.7 µL/min/10⁶ cells</p>
 <p>OSA_837</p> <p>MRSA MIC > 32 µg/mL Aq. Sol. = 317 µM LogD_{7.4} = 1.2 PPB = 60%</p> <p>HLM CLint < 3 µL/min/mg protein Rat Hep CLint < 1 µL/min/10⁶ cells MRC5 TC₅₀ = 14.3 µg/mL PMM TC₅₀ = 21.7 µg/mL SI MRC5 < 0 SI PMM = 1</p>	 <p>OSA_838</p> <p>MRSA MIC > 32 µg/mL Aq. Sol. = 756 µM LogD_{7.4} = 0.9 PPB = 55%</p> <p>HLM CLint < 3 µL/min/mg protein Rat Hep CLint < 1 µL/min/10⁶ cells MRC5 TC₅₀ = 9.3 µg/mL PMM TC₅₀ = 20.7 µg/mL SI MRC5 < 0 SI PMM = 1</p>	 <p>OSA_974</p> <p>MRSA MIC > 32 µg/mL Aq. Sol. = 782 µM LogD_{7.4} = 1.1 PPB = 45%</p> <p>HLM CLint < 3 µL/min/mg protein Rat Hep CLint < 1 µL/min/10⁶ cells MRC5 TC₅₀ = 18.1 µg/mL PMM TC₅₀ = 21.3 µg/mL SI MRC5 = 1 SI PMM = 1</p>	 <p>OSA_859</p> <p>MRSA MIC > 32 µg/mL Aq. Sol. = 178 µM LogD_{7.4} = 3.0</p> <p>HLM CLint = 168 µL/min/mg protein Rat Hep CLint = 49.8 µL/min/10⁶ cells MRC5 TC₅₀ = 3.0 µg/mL PMM TC₅₀ = 9.3 µg/mL SI MRC5 < 0 SI PMM < 0</p>
 <p>OSA_982</p> <p>MRSA MIC = 2 µg/mL Aq. Sol. = 3 µM LogD_{7.4} = 3.6 PPB = 99.3%</p> <p>HLM CLint = 61.8 µL/min/mg protein Rat Hep CLint = 108.0 µL/min/10⁶ cells MRC5 TC₅₀ = 1.5 µg/mL PMM TC₅₀ = 0.7 µg/mL SI MRC5 = 1 SI PMM < 0</p>	 <p>OSA_983</p> <p>MRSA MIC = 2 µg/mL Aq. Sol. = 8 µM LogD_{7.4} = 4.6 PPB = 99.6%</p> <p>HLM CLint = 58.8 µL/min/mg protein Rat Hep CLint = 234.0 µL/min/10⁶ cells MRC5 TC₅₀ = 20.0 µg/mL PMM TC₅₀ = 8.3 µg/mL SI MRC5 = 10 SI PMM = 4</p>	 <p>OSA_978</p> <p>MRSA MIC = 4 µg/mL Aq. Sol. = 5 µM LogD_{7.4} = 3.1 PPB = 99%</p> <p>HLM CLint = 65.6 µL/min/mg protein Rat Hep CLint = 104.0 µL/min/10⁶ cells MRC5 TC₅₀ = 2.0 µg/mL PMM TC₅₀ = 0.6 µg/mL SI MRC5 > 0 SI PMM > 0</p>	 <p>OSA_975</p> <p>MRSA MIC = 4 µg/mL Aq. Sol. = 38 µM LogD_{7.4} = 1.9 PPB = 71%</p> <p>HLM CLint = 99.1 µL/min/mg protein Rat Hep CLint = 7.99 µL/min/10⁶ cells MRC5 TC₅₀ = 7.5 µg/mL PMM TC₅₀ = 18.3 µg/mL SI MRC5 = 2 SI PMM = 5</p>

Figure 3: Human and rat liver microsomes and hepatocyte intrinsic clearance data, and mammalian cell line toxicity results. MRSA MIC data units are µg/mL. SI = ratio of cytotoxic TC₅₀ and MRSA MIC.

Of the initially-studied compounds, the potent benzofuran **821** performed better than the potent benzothiophene **822** (particularly in rat liver microsomes) though it is also known that benzofuran-containing compounds can undergo metabolic activation at the 2-position^{18b} which had made replacement of this functionality a priority for series development. We also confirmed potential sites of metabolism using SMARTCyp (https://smartcyp.sund.ku.dk/mol_to_som, Figure S3 in Supporting Information - Biology).

To probe experimentally the cause of any CYP-mediated metabolic liability in the promising benzofuran, this compound was screened with a PolyCYPs enzyme panel kit (provided by Hypha Discovery) that identified one main monohydroxylated metabolite. This matched the monohydroxylated metabolite observed in human liver S9 incubations in the presence of NADPH cofactor-generating system; human liver S9 incubations performed in the presence of UDP-GA

cofactor resulted in samples containing a directly-conjugated glucuronide metabolite, the structure of which was not determined. (Supplementary Information – Biology). Following a scale-up reaction with one of the PolyCYP enzymes, it was possible to identify the main hydroxylated metabolite (**997**, **Figure 4**) resulting from oxidation on the unsaturated core at the 7-position (Supplementary Information – Chemistry). This metabolite was found to be inactive when evaluated vs. MRSA. The metabolic liability identified for the benzofuran may not be responsible for the intrinsic clearance data obtained, since compounds with such a motif displayed similar intrinsic clearance to analogous compounds with a fully aromatic core (e.g., **865** vs **1018**).

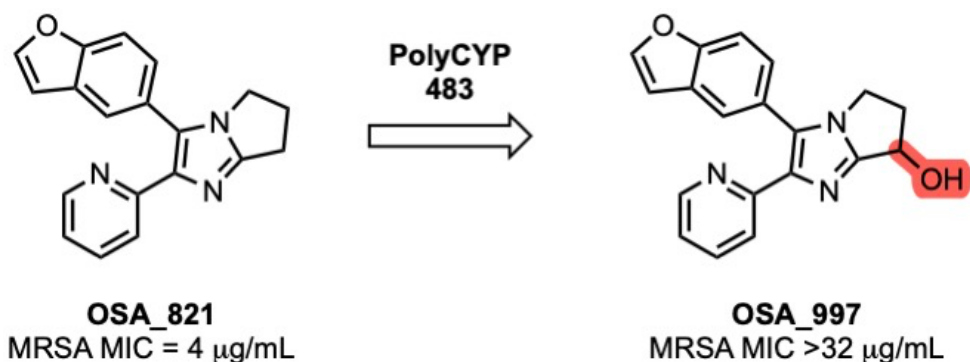


Figure 4. Structure and MRSA activity of a metabolite of **821**.

Several compounds displayed low microsomal intrinsic clearance (e.g., HLM CL_{int} < 3 $\mu\text{g/min/mg}$ protein for **837**, **838** and **974**) in tandem with good solubility, but these compounds were not potent. The fully aromatic (imidazopyridine **1018**) vs partially aromatic (diarylimidazole **865**) cores performed approximately equivalently. The introduction of the nitrogen linker between rings did not have the expected impact on compound solubility (e.g., **859** vs **982**, **982** and **983**).

To judge the selectivity of this series for MRSA vs. other cells, toxicity of key compounds was evaluated against MRC-5_{SV2} (human lung fibroblast cell line) and PMM (primary mouse macrophages) and the selectivity index (SI) calculated (where SI = ratio of cytotoxic TC₅₀ and MRSA MIC; additional data can be found in Table S5 in Supplementary Information – Biology). Most of the inactive compounds exhibited low toxicity to either cell line. The imidazopyridine **983** showed a good selectivity index (SI = 10) for the MRC5 cell line, but this was accompanied by poor ADME properties. The best overall balance of parameters in these systems was found with **975**, a potent compound with reasonable solubility and low intrinsic clearance in rat hepatocytes, with low toxicity against MRC5 cells and no toxicity against PMM.

The importance of balancing potency vs. MRSA and cytotoxicity led us to examine a subset of compounds more thoroughly for toxicity against the human embryonic kidney cell line HEK293. We measure toxicity through either CC₅₀ (concentration of compound inducing 50% reduction in viability) or D_{max} as defined by CO-ADD¹⁹ and calculated following exposure of cells to compounds and recording of metabolic activity *via* either tetrazolium dye absorbance or resofurin fluorescence (methods are described in Supplementary Information – Biology). D_{max} is a parameter which quantifies toxicity at the highest tested concentration (32 $\mu\text{g/mL}$ for all compounds), calculated as reciprocal percentage of viable cells (100 – viability %) where cells were either allowed to recover or viability was measured immediately after treatment. While some studies suggest that 3-[4,5-dimethylthiazol-2-yl]-2,5-diphenyl tetrazolium bromide is less sensitive

than resofurin,²⁰ others report overestimation of viability due to accumulation of resofurin in cells or the opposite due to extensive reduction of the dye by cells with high metabolic activity.²¹ Our efforts focused on trying to replicate the original toxicity experiments (by CO-ADD) with tamoxifen using a protocol modified for use with 96-well plates. Given the variability of protocols and results in the literature²² it was important to compare with a standard protocol we have reliably used in our own laboratory.²³ When both CC_{50} values and D_{max} are mapped against the other two experimental variables (*i.e.*, recovery status after treatment (yes/no) and the detection output (MTT/resazurin)) the majority of compounds were found to be toxic as classified by CO-ADD¹⁹ with a small spread of the data for most variations of protocol used (Figure 5A). Truly “non-toxic” compounds might be expected to show $D_{max} < 50\%$ for all experiment variations, *e.g.*, **861**. The D_{max} spread for the control compound (tamoxifen) across all experiments was small and in agreement with previously-measured values (CC_{50} 9 ± 2 $\mu\text{g/mL}$).¹⁹ A small difference in D_{max} irrespective of whether cells were allowed to recover suggests those compounds are cytostatic or induce a partial response through a mechanism of toxicity which results in slowed cell growth or cause cell death through mechanisms the cells can resist,^{22,24} for example compounds **821**, **822**, **869**, **979**, **982**, **983** and **984**. A large spread of D_{max} values comparing recovery and non-recovery conditions larger than 20% is perhaps indicative of a mechanism of toxicity that persists beyond exposure, *i.e.*, cytotoxic compounds that continue to induce toxicity as cells recover and restart dividing, for example compounds **865**, **870**, **871**, **980** and **981**. CC_{50} values reflect these classifications (Figure 5B) with **861**, **862** and **869** being least toxic compared to tamoxifen (CC_{50} 5.3–15.5 $\mu\text{g/mL}$) while other compounds exhibit CC_{50} values associated with higher toxicity (1–6 $\mu\text{g/mL}$). Where resofurin fluorescence was the measured output, data are more variable (*e.g.*, **862** was found to be non-toxic by both resazurin assay as well as with MTT after recovery, but toxicity more than 50% was measured in the acute exposure by MTT). This variability could be driven by interference of the compounds with the fluorescence readout or resofurin build-up as previously described.²¹ Another limitation to consider is the solubility of the compounds; while all were tested at concentrations ranging from 32 $\mu\text{g/mL}$ (approximately 100 μM for a 300 Da compound) to 0.00625 $\mu\text{g/mL}$ (~ 0.19 μM) with a dilution factor of 2, all compounds screened against HEK293 except for **821**, **861** and **870** have aqueous solubility less than 100 μM . Consequently, compounds precipitating during the assay or unpredictable interactions with serum in the media (and as a result interaction with the cells and their transport in the cell) may explain the spread of the data shown, in particular for those with very low aqueous solubility, such as **983**.

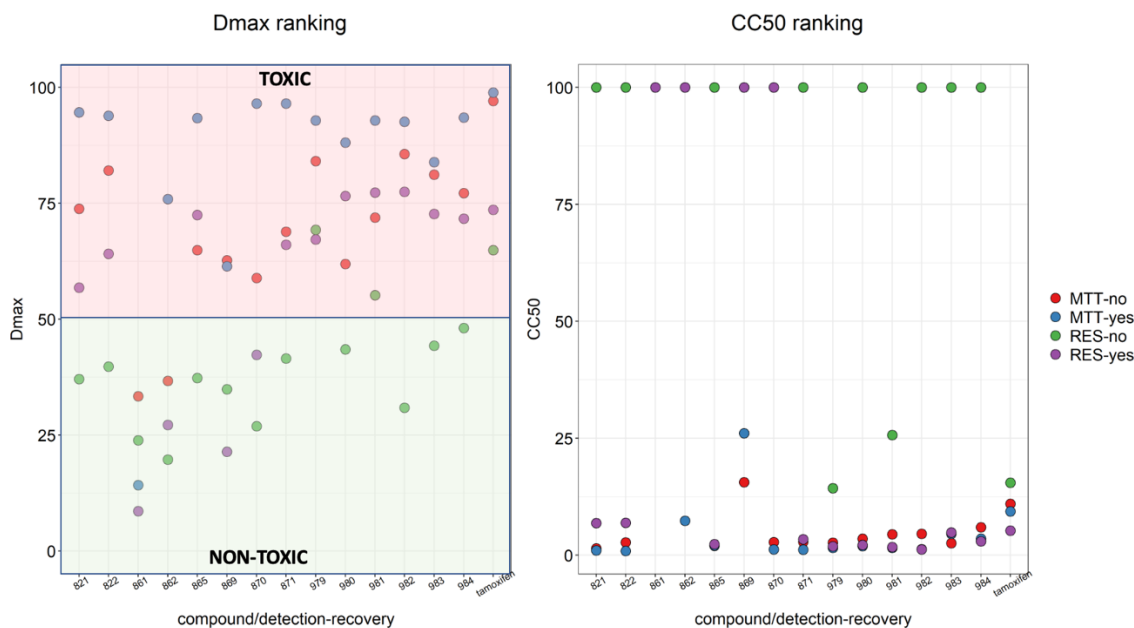


Figure 5. a) D_{\max} classification – compound toxicity at highest concentration is mapped against recovery status and detection output; compounds where D_{\max} is lower than 50% are deemed non-toxic. b) CC_{50} classification – concentrations resulting in 50% reduction in viability were calculated by fitting logistic curves to viability data.

An attempt to characterize the mechanism of toxicity led to testing compound interaction with DNA molecular beacons, which are short strands of DNA tagged with a donor-acceptor pair of fluorophores. The proximity between the fluorophores when the DNA strand is correctly folded results in no fluorescence from the donor; should a compound interfere with DNA folding, a change in melting temperature will be observed. No compounds tested showed reduction in DNA melting temperature (Figure S5 Supplementary Material – Biology), meaning compounds did not interfere with DNA folding. By comparison, doxorubicin showed a dose-response behavior and is a known DNA intercalator.²⁵

Kinase Target Selectivity

To understand the mammalian toxicity of these diarylimidazole derivatives, and to aid in future compound design, we experimentally investigated the potential series mechanism of action (MoA). In the absence of a clear position where we might be able to attach a linker that would permit a pull-down experiment, and because these structures were originally based on known kinase inhibitors, a representative active (**822**) and inactive (**820**) compound were profiled using the MIB-MS (multiplexed inhibitor beads with mass spectroscopic detection) proteomic technique.²⁶ This affinity composition assay has proven to be a useful approach to validate kinase inhibitor selectivity. The results from applying this method to HEK293 cell lysates suggested that TGF- β 1 could potentially be a mammalian target for this series of compounds as with the active compound both kinases were selectively competed off MIBs (1 μ M), whereas similar results were not observed with the inactive compound (Figure 6, see Supplementary Information - Biology for

full data). Whether inhibition of TGF- β 1 contributes to the cytotoxicity observed remains to be determined.

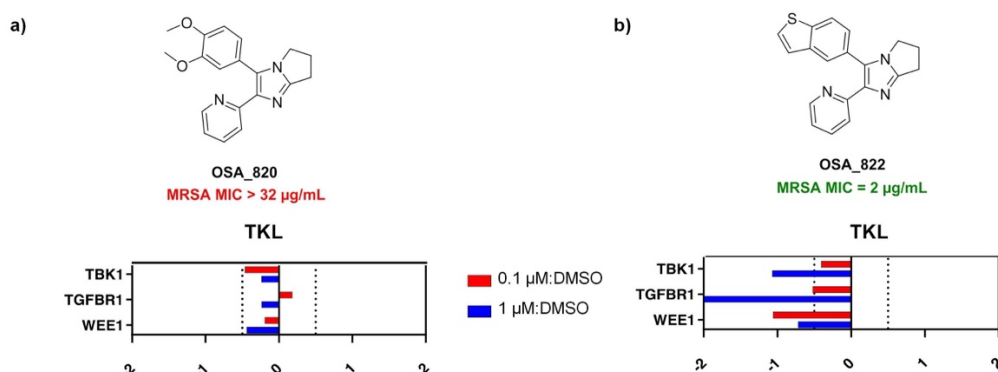


Figure 6. MIBs competition assay reveals potential kinase selectivity in mammalian cells. Shown is a subset of the kinome competition results from incubation of HEK293 cell lysate with compounds **822** (active) and **820** (inactive). Following a brief incubation with these compounds, lysates were passed over MIBs beads (see SI) and the captured kinases identified and quantified by mass spectrometry. Displaced kinases are shown to the left of center line at the designated doses.

Further support for TGF- β 1 being a mammalian target comes from a report of compounds similar in structure to **822** bound to this protein (PDB: 3TZM and 1RW8)²⁷ and the original GSK work on a precursor to this series mentioned above.

Conclusions and Next Steps

Building on publicly available data derived from a CO-ADD screen, we have investigated the promising activity against MRSA of a set of diarylimidazoles. Through synthetic variation of the core structure, we have identified simple molecules with good potency, solubility and low metabolic clearance; the identification of a metabolite was made possible by a private sector contribution to this open research project. Potency tended to correlate with toxicity to mammalian cells, and through experimental investigation of the series' mechanism of action we have identified TGF- β 1 as the potential mammalian target. Two key unanswered questions that could be pursued next for this series include: 1) confirmation of the mechanism of action (both in MRSA, and in mammalian cell lines to explain toxicity) using pull-down experiments with modified versions of the compounds, a strategy requiring the addition of a tether to the structure which, based on the SAR obtained to date, could be installed in place of the methoxy group in **980**, and 2) further analog synthesis rounds based on the most attractive current compound, **975**. Continuation of this research along these lines is made straightforward for the community by the availability of all data and discussions,¹³ and a platform for collaboration, on the Open Source Antibiotics infrastructure.

Acknowledgements

We acknowledge funding from Pharmalliance (a coalition of the School of Pharmacy (University College London), the Eshelman School of Pharmacy (University of North Carolina at Chapel Hill) and the Faculty of Pharmacy and Pharmaceutical Sciences (Monash University)), grant PA2019TierB_ID31. NEU acknowledge funding from the National Institute of Allergy and Infectious Diseases (R33AI141227). We are grateful to Fundação de Amparo à Pesquisa do Estado de São Paulo (FAPESP) for funding (grant numbers: #2017/22001-0 and 2021/11899-0 (DGS)). DNDi is grateful to the French Development Agency (AFD), France for funding the OSN, and to the following donors for contributing to DNDi's overall mission: UK aid, UK; Médecins Sans Frontières, International; and the Swiss Agency for Development and Cooperation (SDC), Switzerland. We thank AstraZeneca for the provision of the *in vitro* ADME and physicochemical properties data included in the manuscript. Antimicrobial screening was performed by CO-ADD (The Community for Antimicrobial Drug Discovery), funded by the Wellcome Trust (UK) and The University of Queensland (Australia). We thank Dr Fahima Idiris (UCL, now Pharmaron), Dr James Callahan (GSK) and Professor Robert Hanson (NEU) for helpful early discussions. A.L-M acknowledges support from the Spanish MECD (FPU 14/00818). The Structural Genomics Consortium (SGC) is a registered charity (no: 1097737) that receives funds from Bayer AG, Boehringer Ingelheim, Bristol Myers Squibb, Genentech, Genome Canada through Ontario Genomics Institute [OGI-196], EU/EFPIA/OICR/McGill/KTH/Diamond Innovative Medicines Initiative 2 Joint Undertaking [EUbOPEN grant 875510], Janssen, Merck KGaA (aka EMD in Canada and US), Pfizer and Takeda.

References

1. (a) Cassini, A.; Högberg, L. D.; Plachouras, D.; Quattrocchi, A.; Hoxha, A.; Simonsen, G. S.; Colomb-Cotinat, M.; Kretzschmar, M. E.; Devleeschauwer, B.; Cecchini, M.; Ouakrim, D. A.; Oliveira, T. C.; Struelens, M. J.; Suetens, C.; Monnet, D. L.; Strauss, R.; Mertens, K.; Struyf, T.; Catry, B.; Latour, K.; Ivanov, I. N.; Dobрева, E. G.; Tambic Andrašević, A.; Soplek, S.; Budimir, A.; Paphitou, N.; Žemlicková, H.; Schytte Olsen, S.; Wolff Sönksen, U.; Mártin, P.; Ivanova, M.; Lyytikäinen, O.; Jalava, J.; Coignard, B.; Eckmanns, T.; Abu Sin, M.; Haller, S.; Daikos, G. L.; Gikas, A.; Tsiodras, S.; Kontopidou, F.; Tóth, Á.; Hajdu, Á.; Guólaugsson, Ó.; Kristinsson, K. G.; Murchan, S.; Burns, K.; Pezzotti, P.; Gagliotti, C.; Dumpis, U.; Liuimiene, A.; Perrin, M.; Borg, M. A.; de Greeff, S. C.; Monen, J. C. M.; Koek, M. B. G.; Elstrøm, P.; Zabicka, D.; Deptula, A.; Hryniewicz, W.; Caniça, M.; Nogueira, P. J.; Fernandes, P. A.; Manageiro, V.; Popescu, G. A.; Serban, R. I.; Schréterová, E.; Litvová, S.; Štefkovicová, M.; Kolman, J.; Klavs, I.; Korošec, A.; Aracil, B.; Asensio, A.; Pérez-Vázquez, M.; Billström, H.; Larsson, S.; Reilly, J. S.; Johnson, A.; Hopkins, S., Attributable Deaths and Disability-adjusted Life-years Caused by Infections with Antibiotic-resistant Bacteria in the EU and the European Economic Area in 2015: a Population-level Modelling Analysis. *Lancet Infect. Dis.* **2019**, *19*, 56–66; (b) CDC. COVID-19: U.S. Impact on Antimicrobial Resistance, S. R. A., GA: U.S. Department of Health and Human Services, CDC; **2022**; (c) Cook, M. A.; Wright, G. D., The Past, Present, and Future of Antibiotics. *Sci. Transl. Med.* **2022**, *14* (657), 10; (d) World Health Organization **2021**, Global Action Plan on Antimicrobial Resistance. <https://www.who.int/publications/i/item/9789240027336> (accessed 6 January, 2022).
2. (a) Devi, S., No Time to Lower the Guard on AMR. *Lancet Microbe* **2020**, *1* (5), e198; (b) Paula, H. S. C.; Santiago, S. B.; Araújo, L. A.; Pedroso, C. F.; Marinho, T. A.; Gonçalves, I. A. J.; Santos, T. A. P.; Pinheiro, R. S.; Oliveira, G. A.; Batista, K. A., An Overview on the Current Available Treatment for COVID-19 and the Impact of Antibiotic Administration During the Pandemic. *Braz. J. Med. Biol. Res.* **2021**, *10* (55).
3. Antibiotics Currently in Global Clinical Development. Philadelphia, PA. Pew Charitable Trusts; 2021. <https://www.pewtrusts.org/en/research-and-analysis/data-visualizations/2014/antibiotics-currently-in-clinical-development> (accessed 6 January, 2022).
4. Årdal, C.; Balasegaram, M.; Laxminarayan, R.; McAdams, D.; Outtersson, K.; Rex, J. H.; Sumpradit, N., Antibiotic Development – Economic, Regulatory and Societal Challenges. *Nat. Rev. Microbiol.* **2020**, *18* (5), 267–274.
5. Klug, D.; Idris, F.; Blaskovich, M.; von Delft, F.; Dowson, C.; Kirchhelle, C.; Roberts, A.; Singer, A.; Todd, M., There is No Market for New Antibiotics: This Allows an Open Approach to Research and Development [version 1; peer review: 3 approved]. *Wellcome Open Res.* **2021**, *6* (146).
6. Todd, M. H., Six Laws of Open Source Drug Discovery. *ChemMedChem* **2019**, *14* (21), 1804–1809.
7. Williamson, A. E.; Ylloja, P. M.; Robertson, M. N.; Antonova-Koch, Y.; Avery, V.; Baell, J. B.; Batchu, H.; Batra, S.; Burrows, J. N.; Bhattacharyya, S.; Calderon, F.; Charman, S. A.; Clark, J.; Crespo, B.; Dean, M.; Debbert, S. L.; Delves, M.; Dennis, A. S. M.; Deroose, F.; Duffy, S.; Fletcher, S.; Giaever, G.; Hallyburton, I.; Gamo, F.-J.; Gebbia, M.; Guy, R. K.; Hungerford, Z.; Kirk, K.; Lafuente-Monasterio, M. J.; Lee, A.; Meister, S.; Nislow, C.; Overington, J. P.; Papadatos, G.; Patiny, L.; Pham, J.; Ralph, S. A.; Ruecker, A.; Ryan, E.; Southan, C.; Srivastava, K.; Swain, C.; Tarnowski, M. J.; Thomson, P.; Turner, P.; Wallace, I. M.; Wells, T. N. C.; White, K.; White, L.; Willis, P.; Winzeler, E. A.; Wittlin, S.; Todd, M. H., Open Source Drug Discovery: Highly Potent Antimalarial Compounds Derived from the Tres Cantos Arylpyrroles. *ACS Central Science* **2016**, *2* (10), 687–701.

8. Lim, W.; Melse, Y.; Konings, M.; Phat Duong, H.; Eadie, K.; Laleu, B.; Perry, B.; Todd, M. H.; Ioset, J.-R.; van de Sande, W. W. J., Addressing the Most Neglected Diseases Through an Open Research Model: The Discovery of Fenarimols as Novel Drug Candidates for *Eumycetoma*. *PLOS Negl. Trop. Dis.* **2018**, *12* (4), e0006437.
9. Zuegg, J.; Hansford, K. A.; Elliott, A. G.; Cooper, M. A.; Blaskovich, M. A. T., How to Stimulate and Facilitate Early Stage Antibiotic Discovery. *ACS Infect. Dis.* **2020**, *6* (6), 1302–1304.
10. COVID-19: U.S. Impact on Antimicrobial Resistance, Special Report 2022. Centers for Disease Control and Prevention, National Center for Emerging and Zoonotic Infectious Diseases, Division of Healthcare Quality, Promotion. <https://dx.doi.org/10.15620/cdc:117915>: Hyattsville, MD, 2022 (accessed 6 January, 2022).
11. Patangia, D. V.; Ryan, C. A.; Dempsey, E.; Ross, R. P.; Stanton, C., Impact of Antibiotics on the Human Microbiome and Consequences for Host Health. *Microbiologyopen* **2022**, *11* (1): e1260.
12. Callahan, J. F.; Burgess, J. L.; Fornwald, J. A.; Gaster, L. M.; Harling, J. D.; Harrington, F. P.; Heer, J.; Kwon, C.; Lehr, R.; Mathur, A.; Olson, B. A.; Weinstock, J.; Laping, N. J., Identification of Novel Inhibitors of the Transforming Growth Factor β 1 (TGF- β 1) Type 1 Receptor (ALK5). *J. Med. Chem.* **2002**, *45* (5), 999–1001.
13. Online notebooks are available through Open Source Antibiotics (<https://github.com/opensourceantibiotics/Series-2-Diarylimidazoles/wiki/Submissions%2C-Resources%2C-and-Data>); offline copies of notebooks are available on the University College London electronic repository at <https://doi.org/10.5522/04/21749750>. Research meeting recordings are available at https://www.youtube.com/playlist?list=PL0eLxnHhou_k1Upbn5X1mdHBwKMYkRpLH using the filter “Series 2.”
14. (a) Silva, D. G.; Junker, A.; de Melo, S. M. G.; Fumagalli, F.; Gillespie, J. R.; Molasky, N.; Buckner, F. S.; Matheussen, A.; Caljon, G.; Maes, L.; Emery, F. S., Synthesis and Structure–Activity Relationships of Imidazopyridine/Pyrimidine- and Furopyridine-Based Anti-infective Agents against Trypanosomiasis. *ChemMedChem* **2021**, *16* (6), 966–975; (b) Silva, D. G.; Gillespie, J. R.; Ranade, R. M.; Herbst, Z. M.; Nguyen, U. T. T.; Buckner, F. S.; Montanari, C. A.; Gelb, M. H., New Class of Antitrypanosomal Agents Based on Imidazopyridines. *ACS Med. Chem. Lett.* **2017**, *8* (7), 766–770.
15. Ansari, A. J.; Sharma, S.; Pathare, R. S.; Gopal, K.; Sawant, D. M.; Pardasani, R. T., Solvent-free Multicomponent Synthesis of Biologically-active Fused–imidazo Heterocycles Catalyzed by Reusable $\text{Yb}(\text{OTf})_3$ Under Microwave Irradiation. *ChemistrySelect* **2016**, *1* (5), 1016–1021.
16. Akao, Y.; Canan, S.; Cao, Y.; Condroski, K.; Engkvist, O.; Itono, S.; Kaki, R.; Kimura, C.; Kogej, T.; Nagaoka, K.; Naito, A.; Nakai, H.; Pairaudeau, G.; Radu, C.; Roberts, I.; Shimada, M.; Shum, D.; Watanabe, N.-a.; Xie, H.; Yonezawa, S.; Yoshida, O.; Yoshida, R.; Mowbray, C.; Perry, B., Collaborative Virtual Screening to Elaborate an Imidazo[1,2-a]pyridine Hit Series for Visceral Leishmaniasis. *RSC Med. Chem.* **2021**, *12* (3), 384–393.
17. Dichiara, M.; Simpson, Q. J.; Quotadamo, A.; Jalani, H. B.; Huang, A. X.; Millard, C. C.; Klug, D. M.; Tse, E. G.; Todd, M. H.; Gedder, D.; da Silva Emery, F.; Carlson, J. E.; Zheng, S.-L.; Vleminckx, M.; Matheussen, A.; Caljon, G.; Pollastri, M. P.; Sjö, P.; Perry, B.; Ferrins, L., Structure-property Optimization of a Series of Imidazopyridines for Visceral Leishmaniasis, *ACS Infect. Dis.* **2023**, *in press* (id-2023-000406, accepted 01-Jun-2023).
18. (a) Gramec, D.; Peterlin Mašič, L.; Sollner Dolenc, M., Bioactivation Potential of Thiophene-Containing Drugs. *Chem. Res. Toxicol.* **2014**, *27* (8), 1344–1358; (b) Kalgutkar, A. S.; Gardner,

- I.; Obach, R. S.; Shaffer, C. L.; Callegari, E.; Henne, K. R.; Mutlib, A. E.; Dalvie, D. K.; Lee, J. S.; Nakai, Y.; O'Donnell, J. P.; Boer, J.; Harriman, S. P., A Comprehensive Listing of Bioactivation Pathways of Organic Functional Groups. *Curr. Drug. Metab.* **2005**, *6* (3), 161–225.
19. Frei, A.; Zuegg, J.; Elliott, A. G.; Baker, M.; Braese, S.; Brown, C.; Chen, F.; Dowson, C. G.; Dujardin, G.; Jung, N.; King, A. P.; Mansour, A. M.; Massi, M.; Moat, J.; Mohamed, H. A.; Renfrew, A. K.; Rutledge, P. J.; Sadler, P. J.; Todd, M. H.; Willans, C. E.; Wilson, J. J.; Cooper, M. A.; Blaskovich, M. A. T., Metal Complexes as a Promising Source for New Antibiotics. *Chem. Sci.*, **2020**, *11*, 2627–2639.
20. Hamid, R.; Rotshteyn, Y.; Rabadi, L.; Parikh, R.; Bullock, P., Comparison of Alamar Blue and MTT Assays for High Through-put Screening. *Toxicol. In Vitro*, **2004**, *18*, 703–710.
21. O'Brien, J.; Wilson, I.; Orton, T.; Pognan, F., Investigation of the Alamar Blue (resazurin) Fluorescent Dye for the Assessment of Mammalian Cell Cytotoxicity. *Eur. J. Biochem.*, **2000**, *267*, 5421–5426.
22. Hafner, M.; Niepel, M.; Chung, M.; Sorger, P. K., Growth Rate Inhibition Metrics Correct for Confounders in Measuring Sensitivity to Cancer Drugs. *Nat. Methods*, **2016**, *13*, 521–527.
23. a) Alley, M. C.; Scudiero, D. A.; Monks, A.; Hursey, M. L.; Czerwinski, M. J.; Fine, D. L.; Abbott, B. J.; Mayo, J. G.; Shoemaker, R. H.; Boyd, M. R., Feasibility of Drug Screening with Panels of Human Tumor Cell Lines Using a Microculture Tetrazolium Assay. *Cancer Res.* **1988**, *48*, 589–601; b) Brown, M. D.; Schätzlein, A.; Brownlie, A.; Jack, V.; Wang, W.; Tetley, L.; Gray, A. I.; Uchegbu, I. F., Preliminary Characterization of Novel Amino Acid Based Polymeric Vesicles as Gene and Drug Delivery Agents. *Bioconjug. Chem.*, **2000**, *11*, 880–891; c) Wong, P. E. E.; Tetley, L.; Dufés, C.; Chooi, K. W.; Bolton, K.; Schätzlein, A. G.; Uchegbu, I. F., Polyamine Aza-Cyclic Compounds Demonstrate Anti-Proliferative Activity In Vitro But Fail to Control Tumour Growth In Vivo. *J. Pharm. Sci.* **2010**, *99*, 4642–4657; d) Brucoli, F.; Natoli, A.; Marimuthu, P.; Borrello, M. T.; Stapleton, P.; Gibbons, S.; Schätzlein, A., Efficient Synthesis and Biological Evaluation of Proximicins A, B and C. *Bioorg. Med. Chem.*, **2012**, *20*, 2019–2024; e) Petkova, A. I.; Kubajewska, I.; Vaideanu, A.; Schätzlein, A. G.; Uchegbu, I. F., Gene Targeting to the Cerebral Cortex Following Intranasal Administration of Polyplexes. *Pharmaceutics*, **2022**, *14*, 1136.
24. Sazonova, E. V.; Chesnokov, M. S.; Zhivotovsky, B.; Kopeina, G. S., Drug Toxicity Assessment: Cell Proliferation versus Cell Death, *Cell Death Discov.*, **2022**, *8*, 417.
25. Pommier, Y.; Leo, E.; Zhang, H.; Marchand, C., DNA Topoisomerases and Their Poisoning by Anticancer and Antibacterial Drugs, *Chem. Biol.*, **2010**, *17*, 421–433.
26. a) McDonald, I. M.; Grant, G. D.; East, M. P.; Gilbert, T. S. K.; Wilkerson, E. M.; Goldfarb, D.; Beri, J.; Herring, L. E.; Vaziri, C.; Cook, J. G.; Emanuele, M. J.; Graves, L. M., Mass Spectrometry-based Selectivity Profiling Identifies a Highly Selective Inhibitor of the Kinase MELK that Delays Mitotic Entry in Cancer Cells, *J. Biol. Chem.* **2020**, *295*, 2359–2374; b) Krulikas, L. J.; McDonald, I. M.; Lee, B.; Okumu, D. O.; East, M. P.; Gilbert, T. S. K.; Herring, L. E.; Golitz, B. T.; Wells, C. I.; Axtman, A. D.; Zuercher, W. J.; Willson, T. M.; Kireev, D.; Yeh, J. J.; Johnson, G. L.; Baines, A. T.; Graves, L. M., Application of Integrated Drug Screening/Kinome Analysis to Identify Inhibitors of Gemcitabine-Resistant Pancreatic Cancer Cell Growth. *SLAS Discov.* **2018**, *23*, 850–861; c) Blake, D. R.; Vaseva, A. V.; Hodge, R. G.; Kline, M. P.; Gilbert, T. S. K.; Tyagi, V.; Huang, D.; Whiten, G. C.; Larson, J. E.; Wang, X.; Pearce, K. H.; Herring, L. E.; Graves, L. M.; Frye, S. V.; Emanuele, M. J.; Cox, A. D.; Der, C. J., Application of a MYC Degradation Screen Identifies Sensitivity to CDK9 Inhibitors in KRAS-mutant Pancreatic Cancer. *Sci. Signal.* **2019**, *12* (590): eaav7259.

27. Ogunjimi, A. A.; Zeqiraj, E.; Ceccarelli, D. F.; Sicheri, F.; Wrana, J. L.; David, L., Structural Basis for Specificity of TGF β Family Receptor Small Molecule Inhibitors. *Cell Signal.* **2012**, *24* (2), 476–483.